Available online at www.sciencedirect.com
ScienceDirect
Journal of Solid State Chemistry 180 (2007) 3076–3081
JOURNAL OF SOLID STATE CHEMISTRY
www.elsevier.com/locate/jssc

Synthesis and luminescent properties of Tb^{3+}-activated yttrium indium germanate phosphor

Yee-Shin Chang[a,*], Hui-Jan Lin[b], Yu-Chun Li[b], Yin-Lai Chai[c], Yeou-Yih Tsai[d]

[a]*Department of Electronic Engineering, National Formosa University, Number 64, Wenhua Road, Huwei, Yunlin 632, Taiwan*
[b]*Department of Materials Science and Engineering, National Cheng Kung University, Tainan 701, Taiwan*
[c]*Department of Resources Engineering, Dahan Institute of Technology, Hualien 971, Taiwan*
[d]*Department of Electronic Engineering, Kao Yuan University Lujhu, Kaohsiung 821, Taiwan*

Received 19 January 2007; received in revised form 25 June 2007; accepted 1 July 2007
Available online 9 August 2007

Abstract

An yttrium indium germanate $YInGe_2O_7$ and $YInGe_2O_7$:Tb^{3+} was synthesized using a vibrating milled solid-state reaction with metal oxides. The structure was characterized by its X-ray powder diffraction pattern. All of the peaks can be attributed to the monoclinic $YInGe_2O_7$ phase, as increasing the Tb^{3+} ion concentrations and the full-width of the half-maximum (fwhm) of these peaks did not cause any obvious differences in the increase in Tb^{3+} concentration. The CIE color coordinates were all in the green region. The phosphor exhibited a bright green emission at 542 nm under excitation at 378 and 258 nm, which belongs to the $^5D_4 \rightarrow {}^7F_5$ transition of Tb^{3+} ions. There were two kinds of emission mechanism in $YInGe_2O_7$:Tb^{3+}: (1) under excitation at 378 nm, time-resolved $^5D_4 \rightarrow {}^7F_5$ transition shows a single exponential decay even when all sites are occupied by Tb^{3+} ions; (2) under excitation at 258 nm, the excited energy was absorbed by the host crystal then transferred effectively to the Tb^{3+} ion which caused the decay curves for the $^5D_4 \rightarrow {}^7F_5$ transition to show non-exponential behavior. There is a maximum value for photoluminescence intensity when the Tb^{3+} concentration is 100 mol% with CIE color coordinates of $x = 0.252$; $y = 0.595$. The concentration quenching effect was not observed, because the $YInGe_2O_7$:Tb^{3+} structure gradually changed to a thortveitite-like structure with increasing Tb^{3+} concentration.

Keywords: Phosphor; Terbium; Photoluminescence; Optical properties

1. Introduction

Over the last decade, luminescent properties of inorganic phosphors have been extensively investigated to make flat panel displays such as field emission displays (FEDs), plasma display panels (PDPs), and thin film electroluminescent devices (TFEL). This process has always been accompanied by improvements in the phosphors used. It is highly desirable to develop novel low-voltage phosphors with high efficiency and chemical stability under electron beam bombardment in a high-vacuum system for the next generation of field emission displays [1,2]. A lot of effort has been put into discovering host materials as well as activators with high performance for phosphor applications [3,4]. Traditional phosphors are rare earth or transition-metal-activated sulfides such as ZnS, SrS, and CaS. Intrinsic problems, such as chemical instability and sensitivity to moisture, make it difficult to pattern the phosphors in films using chemical etching or photolithography [5–7].

Yttrium indium germanate has a thortveitite structure with symmetry described by the space group $C2/m$ (No. 12). This crystallizes in the monoclinic system, with cell parameters: $a = 6.8286$ Å, $b = 8.8836$ Å, and $c = 4.9045$ Å. The In^{3+} and Y^{3+} cations occupy the same octahedral site forming a hexagonal arrangement on the *ab* planes [8]. In turn, the hexagonal arrangements of InO_6/YO_6 octahedral layers are held together by sheets of isolated diorthogroups constituted by a double tetrahedral sharing a common vertex.

Tb^{3+}-activated green phosphors have been used in three-band fluorescent lamps (e.g., (Ce,Gd)MgB_5O_{10}:Tb^{3+} [9]),

*Corresponding author. Fax: +886 5 6315643.
E-mail address: yeeshin@nfu.edu.tw (Y.-S. Chang).

0022-4596/$ - see front matter © 2007 Elsevier Inc. All rights reserved.
doi:10.1016/j.jssc.2007.07.018

projection television tubes (e.g., $Y_3Al_5O_{12}$:Tb^{3+} [10]), and X-ray intensifying screens (e.g., Gd_2O_2S:Tb^{3+} [11]). The optical properties of Tb^{3+} in different host matrices have been extensively studied [12–14]. In view of its intense luminescence in the visible region, transitions from $^5D_3$ and $^5D_4$ to the ^7F_J multiple ground states have been proposed.

The discussion above suggests that $YInGe_2O_7$ possesses excellent optical properties, but the properties of the rare earth Tb^{3+} ion doped in $YInGe_2O_7$ have not yet been studied. In this investigation, Tb^{3+} ion doped yttrium indium germanate phosphors were synthesized using the vibrating milled solid-state reaction. The structure and the photoluminescence properties of $YInGe_2O_7$ and $YInGe_2O_7$:Tb^{3+} phosphors were also investigated.

2. Experimental procedures

2.1. The preparation of samples

The Tb^{3+}-doped $YInGe_2O_7$ was prepared by a vibrating milled solid-state reaction using Y_2O_3, In_2O_3, GeO_2, and Tb_4O_7 powders. Starting materials with the purity of 99.99% were supplied by Aldrich Chemical Company and Alfa Aesar. After being mechanically activated by grinding in a high-energy vibro-mill for 15 min with zirconia balls in a polyethylene jar, the mixture was heated at 1300 °C in air for 10 h. The heat-treated powder was then fired under a reducing atmosphere (3% H_2/97% Ar) at 700 °C to covert Tb^{4+} to Tb^{3+} to obtain higher emission intensity.

2.2. Characterization

The effects of Tb^{3+} doping and thermal treatment on the structure were carefully studied using X-ray powder diffractometry (XRD, Rigaku Dmax-33 X-ray diffractometer) with Cu$K\alpha$ radiation with a source power of 30 kV and a current of 20 mA to identify the possible phases formed after heat treatment. Optical absorption spectra were measured at room temperature using a Hitachi U-3010 UV–vis spectrophotometer. Both excitation and luminescence spectra of these phosphors were recorded on a Hitachi F-4500 fluorescence spectrophotometer using a 150 W xenon arc lamp as the excitation source at room temperature.

3. Results and discussion

3.1. Phases in samples

Fig. 1 shows the X-ray powder diffraction pattern of $YInGe_2O_7$ doped with various concentrations of Tb^{3+} heated at 1300 °C in air for 10 h. All of the peaks can be attributed to the monoclinic $YInGe_2O_7$ phase. The full-width of the half maximum (fwhm) of these peaks did not show any obvious differences with an increase in Tb^{3+} concentrations as the trivalent terbium ions (0.923 Å) [15] are introduced to substitute the trivalent yttrium ions

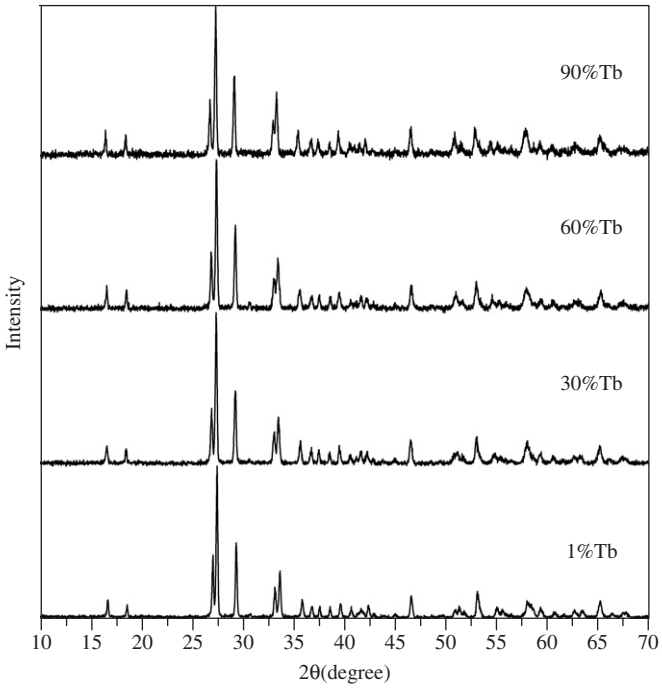

Fig. 1. XRD profiles of $YInGe_2O_7$ doped with various contents of Tb^{3+} heated at 1300 °C for 10 h in air.

(0.9 Å) [15] in the (Y,Tb)$InGe_2O_7$ system. The differences are almost the same for Tb^{3+} and Y^{3+} ion radii which formed a solid solution, indicating that the grain sizes do not change significantly with an increase in Tb^{3+} concentrations. Additionally, there were no charge compensation issues for the Tb^{3+} ions substituting the Y^{3+} ions in the $YInGe_2O_7$ lattice, as both have the same valence.

3.2. Absorption spectrum

Trivalent terbium with a $4f^8$ configuration has complicated energy levels and various possible transitions between f levels. The transitions between these f levels are highly selective and have a sharp line spectra. The optical absorption spectrum measured at room temperature of $YInGe_2O_7$ doped with different Tb^{3+} concentrations is shown in Fig. 2. The absorption bands are at about 200–280 and 280–450 nm. According to the studies by Blasse et al. [16–18], metal ions with a d^{10} configuration show a strong absorption peak in the ultraviolet region. The In^{3+} ion possesses a $4d^{10}$ configuration in which the series of absorption bands between 200 and 280 nm correspond to the charge transfer between In^{3+} and O^{2-} ions of the InO_6 anion in the host lattice. The absorption behavior between 280 and 450 nm is caused by the oxygen deficient center of the GeO_4 anion [19]. It is worth mentioning that typical Tb-activated phosphors show strong $4f$–$5d$ transition band absorption around 200–300 nm [20]. The major absorption edge of pure $YInGe_2O_7$ is in the deeper UV region situated at

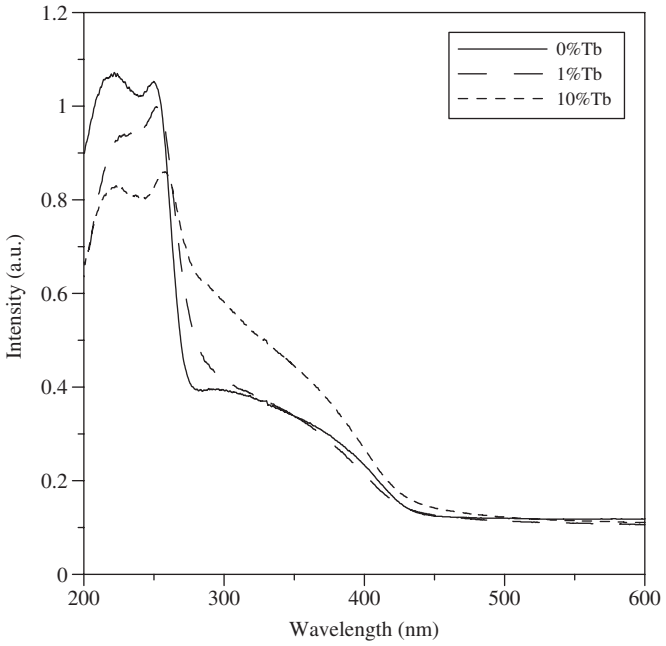

Fig. 2. Absorption spectra of undoped and 1 mol%, 10 mol% Tb-doped $YInGe_2O_7$ powders heated at 1300 °C for 10 h.

~260 nm, and it might be possible that the 4*f*–5*d* transition band overlaps the absorption band of the host lattice and causes the 4*f*–5*d* transition band absorption phenomenon to be undetectable for Tb-activated phosphors [20].

3.3. Excitation and emission spectrum

Fig. 3 is the photoluminescence excitation spectra of $YInGe_2O_7$ doped with different Tb^{3+} ion concentrations heated at 1300 °C for 10 h ($\lambda_{em} = 542$ nm). Of particular interest are the intensities of *f*–*d* transitions being stronger than those of *f*–*f* transitions at lower Tb^{3+} concentrations ($x \leqslant 0.1$), and the intensities of *f*–*d* transitions being weaker than those of *f*–*f* transitions at higher Tb^{3+} concentrations ($x > 0.1$). It is caused by the *f*–*f* transitions type are forbidden and the *f*–*d* transitions type are allowed according to the Laporte's rule [21].

According to the analysis of the excitation spectrum, the strongest excitation wavelength is present at 258 and 378 nm for lower and higher Tb-doped concentrations, respectively, so 258 and 378 nm were chosen to be the excitation wavelengths at which the emission behavior for $YInGe_2O_7$:Tb^{3+} phosphors was observed. Fig. 4 is the photoluminescence emission spectra of pure $YInGe_2O_7$ (dot line) and $YInGe_2O_7$:1 mol% Tb (solid line) at 1300 °C for 10 h under excitation at 258 nm. Samples with various excitation wavelengths had a similar emission spectra pattern to those in Fig. 4. However, there are large differences in excitation behavior between pure and $YInGe_2O_7$-doped Tb^{3+} ions under excitation at 258 nm. When $\lambda_{ex} = 258$ nm, the emission wavelength for pure $YInGe_2O_7$ was located around 350–600 nm, which corre-

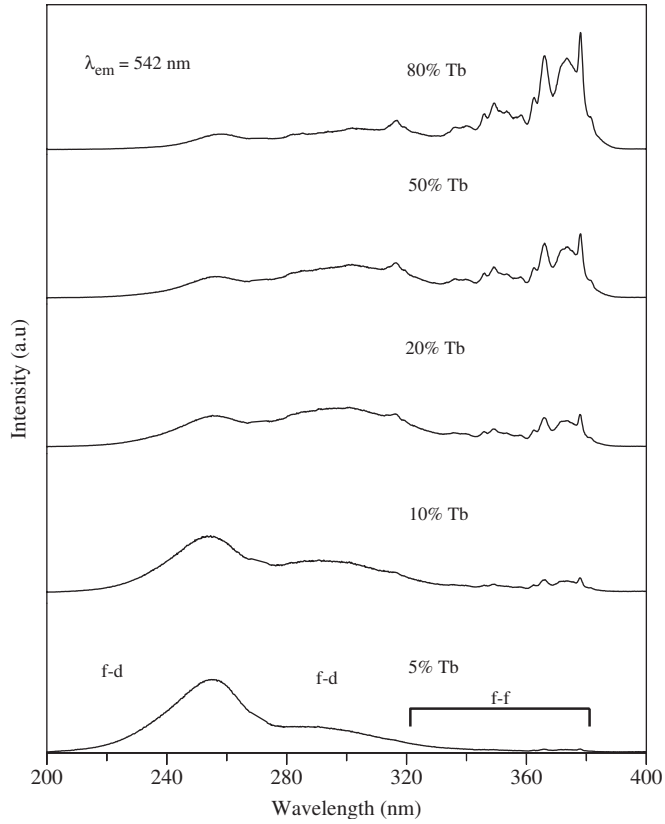

Fig. 3. Photoluminescence excitation spectra of $YInGe_2O_7$:Tb with different Tb^{3+} concentration heated at 1300 °C for 10 h ($\lambda_{em} = 542$ nm).

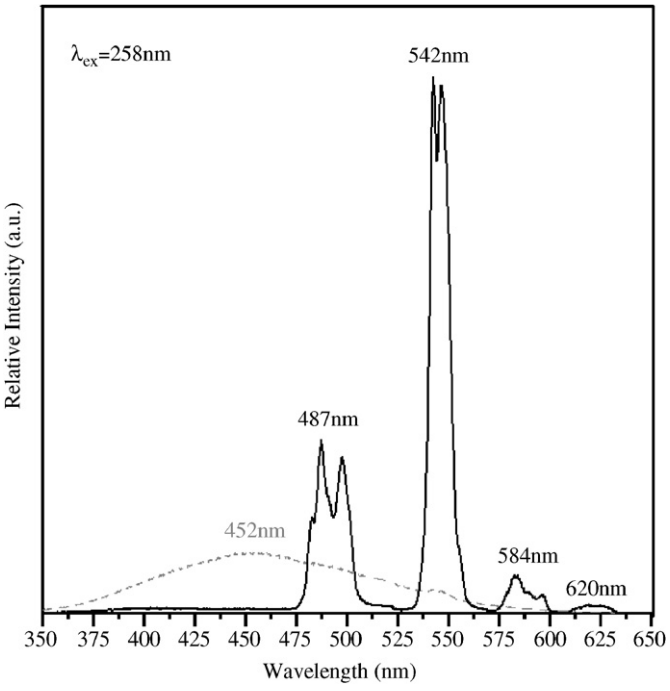

Fig. 4. Photoluminescence emission spectra of pure $YInGe_2O_7$ (dot line) and $YInGe_2O_7$:1 mol% Tb (solid line) heated at 1300 °C for 10 h ($\lambda_{ex} = 258$ nm).

sponds to the charge transfer process from O^{2-} to In^{3+} within the InO_6 octahedra [16,18]. For $YInGe_2O_7$:1 mol% Tb, the characteristic emission peaks located at 487, 542, 584, and 620 nm correspond to the Tb^{3+} intra-4*f* transition from the excited levels to lower levels; the $^5D_4 \rightarrow {}^7F_J$ ($J = 6$, 5, 4, 3) transitions, respectively. In general, at high Tb^{3+} concentrations, the higher energy level emission can be quenched in favor of the lower energy level emission [22]. The following cross-relaxation may occur:

$$Tb^{3+}(^5D_3) + Tb^{3+}(^7F_6) \rightarrow Tb^{3+}(^5D_4) + Tb^{3+}(^7F_0) \quad (1)$$

Luminescence from the higher excited states, such as $^5D_3$, was not detected, indicating a very efficient non-radiative relaxation to the lowest excited $^5D_4$ level. Moreover, there was no emission peak present for the host in the $YInGe_2O_7$:1 mol% Tb emission spectra, indicating that the energy transfers directly from the host to the Tb^{3+} ion. At the start, the excited energy was absorbed by the host crystal and then transferred to the Tb^{3+} ion from the In–O bond because the 4*f*–5*d* transition band overlaps the absorption band of the host lattice, causing luminescence only from the Tb^{3+} ion, a process which is called 'Host Sensitized'.

Fig. 5 shows the photoluminescence emission intensity versus Tb concentrations under an excitation wavelength of (a) 378 nm and (b) 258 nm. In Fig. 5(a), the emission intensity increases with increasing Tb^{3+} concentration and the concentration quenching phenomenon is not observed. There is a maximum value when $YInGe_2O_7$ is doped with 100 mol% Tb^{3+} ions, which is called a stoichiometric phosphor [22]. According to the study by Juarez-Arellano et al. [23], $TbInGe_2O_7$ has a thortveitite-like structure with the space group $C/2c$. Compared with $YInGe_2O_7$, which has a thortveitite structure with space group $C/2m$, the O1 oxygen presents a degree of freedom along the *b*-axis. This degree of freedom allows the angle Ge–O–Ge to change from 180° (thortveitite structure) to 156.8(2)° (thortveitite-like structure). The reason for the change in space group with the increase in Tb content is the increase in the distortion of the polyhedra, which allows a larger degree of freedom. The degree of freedom for the $YInGe_2O_7$:Tb^{3+} structure gradually increases with increasing Tb^{3+} ion concentration, which might enhance the limit for the concentration quenching effect. Therefore, the concentration quenching effect is not observed even though at a Tb^{3+} concentration of 100 mol%. The emission intensity in Fig. 5(b) of the ^5D level decreases rapidly when the Tb^{3+} concentration increases to 10 mol%, and then decreases slightly. It might be caused by the distances between oxygen deficiency and Tb^{3+} ion decreased with increasing the Tb^{3+} ion concentrations, and which led to the interaction between oxygen deficiency and Tb^{3+} ion increased. It caused the sample excitation at 258 nm was absorbed by this parasite band, and decreased the emission efficiency.

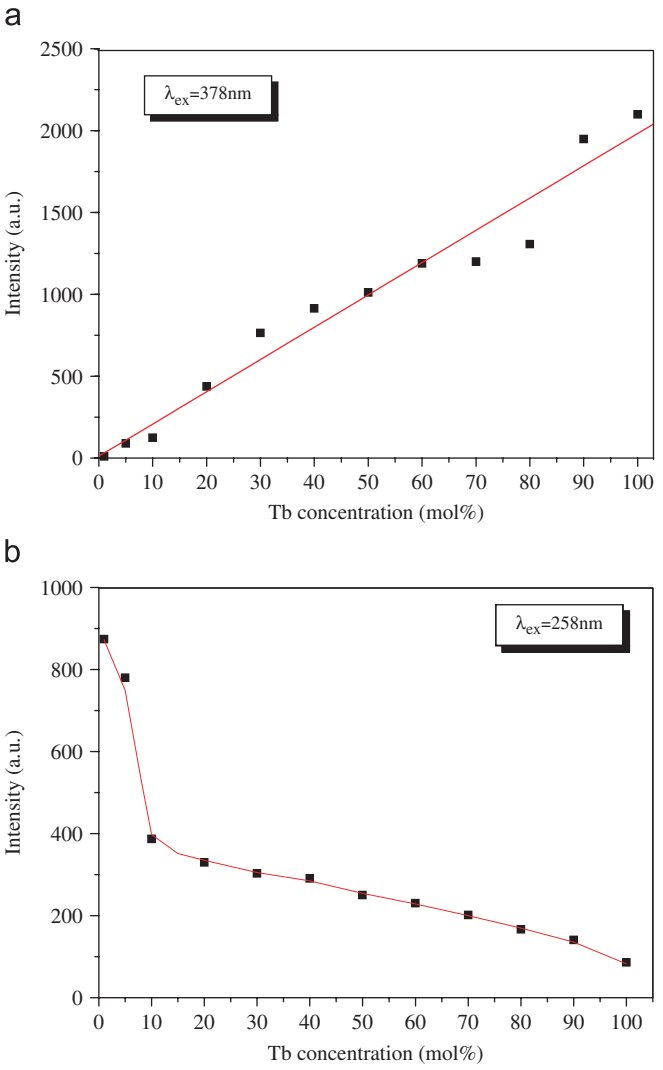

Fig. 5. Photoluminescence emission intensity versus Tb^{3+} concentrations under the excitation wavelength at (a) 378 nm and (b) 258 nm.

3.4. Decay curve and decay time

The luminescence intensity and decay time of phosphor materials are always dependent on the doping concentrations. Fig. 6 shows the luminescent intensity of the $^5D_4 \rightarrow {}^7F_5$ transition in terms of Tb^{3+} concentrations in $YInGe_2O_7$:Tb^{3+} powders under excitation at (a) 378 nm and (b) 258 nm, with signals detected at 542 nm. The decay curves can be represented by [24]

$$I = I_0 \exp\left(\frac{-t}{\tau}\right), \quad (2)$$

where I and I_0 are the luminescence intensities at time t and 0, respectively, and τ is the radiative decay time.

In Fig. 6(a), the decay curves obviously decrease with increasing Tb^{3+} concentration, which is caused by the effect of energy exchange between Tb^{3+} ions as the distance between Tb^{3+} ions decreases with increasing Tb^{3+} ion concentrations. This enhances the depletion rate of energy and causes the decay time to decrease. Time-resolved

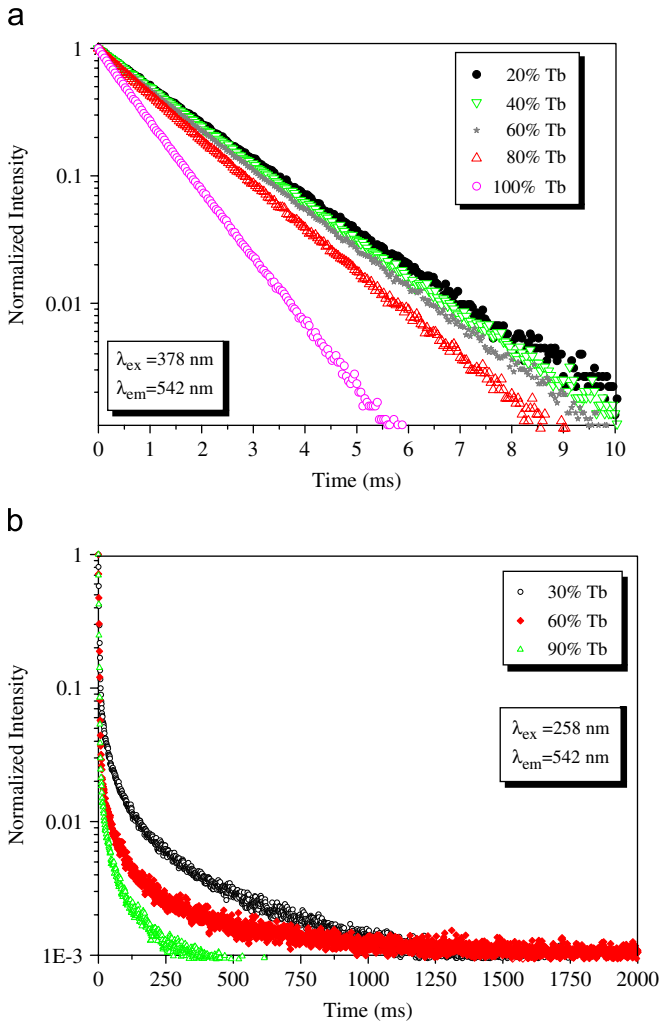

Fig. 6. The decay curve of $YInGe_2O_7$ doped with different Tb^{3+} concentrations under excitation at (a) 378 nm and (b) 258 nm. The signals were detected at 542 nm.

$^5D_4 \rightarrow {}^7F_5$ transition shows a single exponential decay even when all sites are occupied by Tb^{3+} ions. All these curves can be well fitted into a mono-exponential decay, revealing that the presence of the Tb^{3+} environment is unique in accordance with the crystal structure and the decay mechanism of $^5D_4 \rightarrow {}^7F_5$ transition is a single decay component between Tb^{3+} ions only [25,26].

Fig. 6(b) is the decay curve of various Tb^{3+} ion concentrations in $YInGe_2O_7$ under excitation at 258 nm. The results indicate that the decay time decreases from 1250 to 250 ms with increasing Tb^{3+} concentration from 30 to 90 mol%. In contrast, with excitation at 378 nm, the decay curves are obviously different. The observed decay curves were non-exponential, and the non-exponential change becomes more prominent as content increases, revealing that more than one relaxation process exists. Moreover, the decay times are much longer than those when excited at 378 nm. As discussed earlier, the excitation energy was originally absorbed by the host crystal and then transferred effectively to the Tb^{3+} ion, which caused the decay curves to have non-exponential behavior and enhanced the decay time.

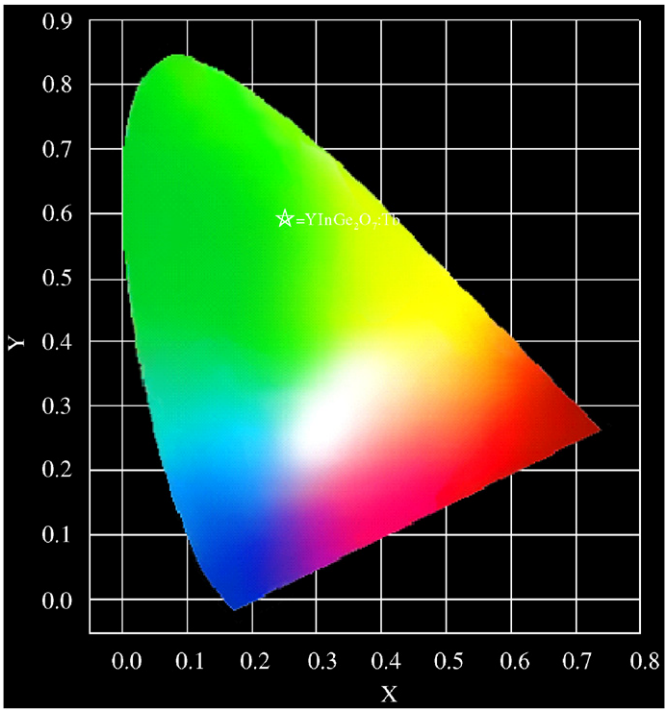

Fig. 7. CIE color coordinate diagram of $YInGe_2O_7$:Tb^{3+} phosphors.

In $YInGe_2O_7$:Tb^{3+}, different concentrations of Tb^{3+} ion doping did not change the wave shape, but did change the intensities for the excitation spectra. Fig. 7 shows the CIE color coordinates of $YInGe_2O_7$:100 mol% Tb, which are in the green region ($x = 0.252$; $y = 0.595$).

4. Conclusions

A new green emitting phosphor, Tb^{3+}-doped $YInGe_2O_7$, shows a bright green emission at 542 nm under excitation at 258 and 378 nm, which belongs to the $^5D_4 \rightarrow {}^7F_5$ transition of Tb^{3+} ions. Two kinds of emission mechanism were observed in $YInGe_2O_7$:Tb^{3+}; in the first, the time-resolved $^5D_4 \rightarrow {}^7F_5$ transition is a single exponential decay between Tb^{3+} ions only at 378 nm, and in the second, the excitation energy is originally absorbed by the host crystal and then transferred effectively to the Tb^{3+} ion, which causes the decay curves for the $^5D_4 \rightarrow {}^7F_5$ transition to have non-exponential behavior at 258 nm. There is a maximum value for photoluminescence intensity when Tb^{3+} concentration is 100 mol% with CIE color coordinates of $x = 0.252$; $y = 0.595$. The concentration quenching effect was not observed because the $YInGe_2O_7$:Tb^{3+} structure changed to a thortveitite-like structure with increasing Tb^{3+} concentrations.

Acknowledgments

The authors would like to thank the National Science Council of the Republic of China for financially supporting this research under Contract no. NSC95-2218-E-150-003.

References

[1] R.Y. Lee, F.L. Zhang, J. Penczek, B.K. Wagner, P.N. Yocom, C.J. Summers, J. Vac. Sci. Technol. B 16 (1998) 855.
[2] S. Yang, C. Stoffers, F. Zhang, S.M. Jacobsen, B.K. Wagner, C.J. Summers, Appl. Phys. Lett. 72 (1998) 158.
[3] K.Y. Kim, H.K. Jung, H.D. Park, D. Kim, J. Lumin. 99 (2002) 169.
[4] Q.Y. Zhang, K. Pita, W. Ye, W.X. Que, Chem. Phys. Lett. 351 (2002) 163.
[5] S. Itoh, H. Toki, K. Morimoto, T. Kishino, J. Electrochem. Soc. 138 (1991) 1509.
[6] S. Itoh, M. Yokoyama, K. Morimoto, J. Vac. Sci. Technol. A 5 (1987) 3430.
[7] S. Itoh, T. Kimizuka, T. Tonegawa, J. Electrochem. Soc. 136 (1989) 1819.
[8] E.A. Juarez-Arellano, L. Bucio, J.L. Ruvalcaba, R. Moreno-Tovar, J.F. Garcia-Robledo, E. Orozco, Z. Kristallogr. 217 (2002) 201.
[9] T.J. ustel, H. Nikol, C. Rhonda, Angew. Chem. Int. Ed. 37 (1998) 3084.
[10] K. Ohno, T. Abe, J. Elctrochem. Soc. 133 (1986) 638.
[11] J.A. de Pooter, A.B. Bril, J. Electrochem. Soc. 122 (1975) 1086.
[12] W.F. van der Weg, T.J.A. Popma, A.T. Vink, J. Appl. Phys. 57 (1985) 5450.
[13] R.P. Rao, W.W. Duley, J. Mater. Sci. 27 (1992) 5883.
[14] M. Nikl, R. Morlotti, C. Magro, R. Bracco, J. Appl. Phys. 79 (1996) 2853.
[15] R.D. Shannon, Acta Crystallogr. A 32 (1976) 751.
[16] G. Blasse, L.H. Brixner, Mater. Chem. Phys. 28 (1991) 275.
[17] G. Blasse, G.J. Dirksen, N. Kimizuka, T. Mohri, Mater. Res. Bull. 21 (1986) 1057.
[18] G. Blasse, Chem. Phys. Lett. 175 (1990) 237.
[19] D.P. Poulios, J.P. Spoonhower, N.P. Bigelow, J. Lumin. 101 (2003) 23.
[20] S. Kubota, T. Endo, J. Electrochem. Soc. 142 (1995) 4269.
[21] D.R. Vij, Luminescence of Solids, Plenum Press, New York, 1998, p.98.
[22] S. Shionoya, W.M. Yen, Phosphor Handbook, CRC Press, Boca Raton, FL, 1999, p. 185.
[23] E.A. Juarez-Arellano, L. Bucio, J.A. Hernandez, E. Camarillo, R.E. Carbonio, E. Orozco, J. Solid State Chem. 170 (2003) 418.
[24] D.R. Vij, Luminescence of Solids, Plenum Press, New York, 1998, p.68.
[25] G. Blasse, B.C. Grabmaier, Luminescent Materials, Springer, New York, 1994, p.96.
[26] Y. C Li, Y.H. Chang, Y.F. Lin, Y.S. Chang, Y.J. Lin, Electrochem. Solid State Lett. 9 (8) (2006) H74.